JOURNALS

# The 3-dimensional thermal analysis for the Keyhole plasma arc welding Technique

***Subramaniyan Raj[1], Rama iyer[2]***
[#1]Department of Mechanical Engineering, subramaniyan Raj Er. Perumal Manimekalai College of Engineering, Hosur, Tamilnadu, India
subramaniyanraj@yahoo.com

***Abstract***
*The evolution of temperature profiles and weld pool geometry in the course of distinct welding among 2205 duplex stainless steel and A36 low carbon metal the use of keyhole plasma arc welding has been simulated the use of a three dimensional numerical warmness switch and fluid go with the flow model. An adaptive warmth supply is proposed as a heat supply model for acting a non-linear temporary thermal evaluation, based totally on the configuration function of keyhole plasma arc welds. Temperature profiles and solidified weld pool geometry are provided for three welding warmth enter. The reversed bugle form parameters (width of fusion zone at both pinnacle and bottom surfaces) of the weld pool geometry capabilities for a multiple 2205–A36 weld joint are summarized to effectively provide an explanation for the observations. The model become additionally applied to keyhole plasma welding of 6.eight mm thick similar 2205 duplex stainless steel joint for validation. The simulation effects have been compared with independently received experimental statistics and excellent agreements have been obtained.*

***Keywords****: diverse metals, finite detail evaluation, weld geometry, temperature area.*

## INTRODUCTION

Duplex stainless steels (DSSs) are gaining appreciably elevated applications as structural materials in various business sectors, consisting of offshore creation, chemical, petrochemical, pulp and paper, energy era, desalination, and oil and fuel. DSSs have advanced mechanical homes and corrosion characteristics relative to other stainless steels and structural steels. Recently, in view of increasing packages of DSSs, it's miles crucial to have a higher understanding of the troubles associated with welds to varied metals. Welding the distinct metals remains extra difficult than that of comparable metals due to the distinction in the physical, mechanical, and metallurgical homes of the metals to be joined. Proper selection of system, and technique parameters are, therefore, mandatory to make the welds with accurate nice. all through traditional fusion welding approaches of DSSs joints, the fabric is subjected to very high heating and cooling prices, that has unfavorable considerable have an impact on the weld excellent. For this reason, plasma arc welding (PAW) of DSSs joints unearths increasing demand due to the decrease cooling charges and with the blessings of excessive welding velocity providing higher productivity. The most generally used approach of PAW is the keyhole mode(Fig.1).

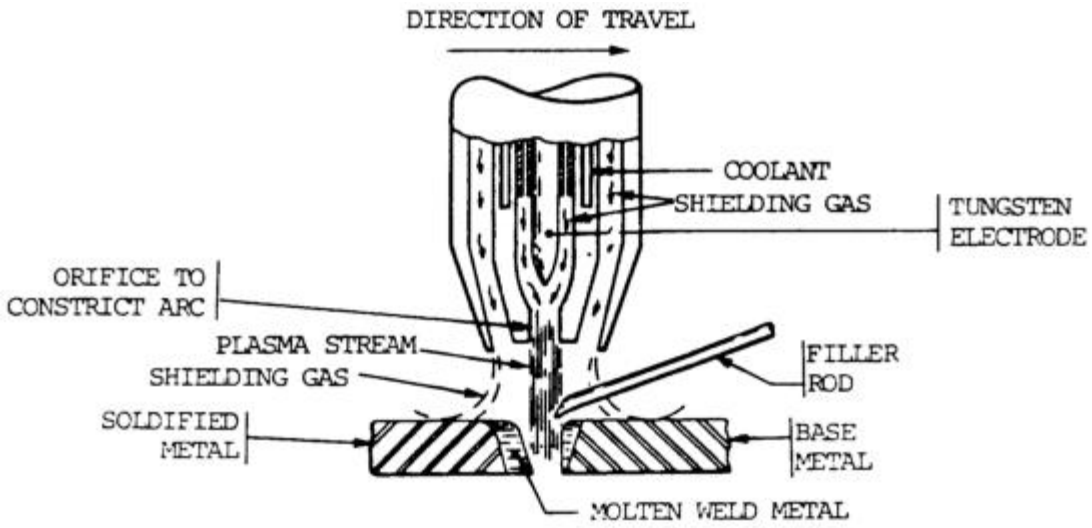


***Fig 1.*** *Process diagram- Keyhole PAW*

The keyhole PAW gives enormous blessings over traditional tungsten inert gas (TIG) welding in terms of penetration intensity, joint practice and thermal distortion. similarly, the keyhole PAW may be used for butt welds from about 3 mm up to 7-8 mm thick with a unmarried pass; by means of contrast, the TIG method is best appropriate for butt welds up to about 3-4mm thick [1]. these are a number of the motives justifying the substitution of TIG welding with plasma keyhole welding. The temperature profile around the keyhole and the weld pool has an extraordinary have an effect on the formation and balance of the keyhole. Therefore, it is of high-quality importance to model and simulate the temperature distribution, weld thermal cycles ,and weld pool geometry in the keyhole PAW technique for distinctive DSSs joints.

**State of the artwork**

In recent years, plasma welding of duplex stainless steels has end up of superb hobby in the enterprise; however, the research woks in this discipline are extraordinarily constrained. Urena et al. [2] have determin ed the top-rated welding situations, in phrases of heat enter, microstructure, and hardness, for plasma welding of 2205 DSS that is 3 mm thick. Zheng et al.[3] have investigated the effects of a twintorch met hod the use of plasma welding observed by TIG welding on the microstructure and corrosion properties of 2205 DSS. Taban [4] investigated the results of plasma welding and of combined plasma and TIG welding at the microstructure and durabilit y of SAF 2205 DSS. In addition paintings, Taban [5] investigated the effect of plasma welding at the durability of united states32750 wonderful duplex chrome steel. Migiakis et al. [6] focused on plasma keyhole welding of americaS32760 (Zeron 100) high-quality duplex stainless steel and studied the microstructure, tensile stre ngth, and impact longevity of the elements . Barnhouse and Lippold [7] have investiga ted the effect of filler metals the usage of TIG welding on the ferrite wide variety of the diverse DSS SAF 2205/carbon steel ASTM-A36 weld joint. Mendoza et al. [8] studied the results of the welding designs and the filler steel on the mechanical residences and micro structural adjustment of distinct superb DSS 2507/API X52 weld joints. Keanini and Rubinsky [9] employed three-D finite detail primarily based simulation of the plasma arc

welding manner to take a look at the effect of the plate ambient temperature at the weld pool's 3-dimensional capillary surface shape and temperature fields. Fan and Kovacevic [10] advanced a mathematical model to describe the heat switch and fluid flow in desk bound keyhole plasma arc welding. Wu et al. [11] advanced a 3-dimensional finite element version for keyhole plasma arc welding and concluded that a changed 3-dimensional conical heat source version is the correct model to mirror the nonlinear decay of the warmth depth distribution along the route of the work piece thickness. In some other paper, Wu et al. [12] hired an adaptive heat supply version for keyhole PAW that blended a double ellipsoidal volumetric warmness supply and a cylindrical volumetric warmth supply. Wang et al. [13] simulated the keyhole PAW through a 3-d FE version and investigated the results of work piece thicknesses at the moments of keyhole formation, and solid keyholes have been analyzed. even though many studies had been performed for welding of 2205 duplex stainless steel, most of the outcomes have been involved with the microstructure and corrosion residences of the welded joints. similarly, studies has been limited to experimental work. there may be a paucity of reliable facts approximately thermal cycles and temperature distributions in multiple 2205 duplex stainless-steel weldments. No attempt has been made yet to simulate 3 dimensional-dimensional finite detail model for keyhole PAW of distinctive 2205–A36 joint.

In this paper, dynamic evolution of geometrical form, the scale and fluid flow of the molten pool, temperature distributio ns and thermal cycles, and the keyhole of multiple 2205–A36 joint have been simulated via the 3-dimensional thermal keyhole PAW finite detail model primarily based at the adaptive warmth supply model proposed through Wu et al. [12]. further, the advanced thermal version has been experimentally confirmed via comparing the anticipated weld pool geometry and size received from the thermal evaluation with the experimental results.

**Finite element evaluation**

In the cutting-edge research, the temperature area and the weld pool geometry all through keyhole PAW of a 2205–A36 plate changed into simulated by using a complete 3-dimensional uncoupled thermal finite detail system that became implemented in ABAQUS® code [14]. For correct simulation of the temperature records, it's miles vital to enforce an extra user-subroutine as a FORTRAN code. The simulated welding parameters are given in table 1.

Table 1. Welding conditions for 6.8 mm thick similar and dissimilar plates

| | 2205/ 2205 | 2205/ A36 | 2205/ A36 | 2205/ A36 |
|---|---|---|---|---|
| Welding current (A) | 140 | 140 | 140 | 140 |
| Arc Voltage (V) | 28 | 28 | 28 | 28 |
| Welding Speed (mm/min) | 120 | 105 | 120 | 135 |
| Arc efficiency | 0.5 | 0.5 | 0.5 | 0.5 |
| heat input (kJ/mm) | 1.96 | 2.25 | 1.96 | 1.75 |
| Ambient temperature (K) | 294 | 294 | 294 | 294 |

The simulation of the system of welding has been executed on a 2205–A36 plate butt joint; the dimensions of the plate is one hundred sixty mm × one hundred sixty mm and the thickness is 6.8 mm. to supply properly-graded finite element meshes that reduce the computation time, the geometri cal models had been partitioned into diverse areas. each vicinity consisted of meshes of various densities. within the vital fusion place near the joint intersectio n region, wherein the temperature gradient s are anticipated to be the most severe,

exceptional meshes were generated. Conversely, regions away from the weld are meshed with a rough mesh. between the refined and the some distance-area regions, transition areas had been used. The 3D symmetrical graded mesh of the welded plate supplied in Fig. 2 reduces the computation time as compared with an ungraded mesh. the overall symmetrical plate model has 195840 8-node linear hexahedral elements and 221531 nodes. 8-node three-D hexahedral elements of the ABAQUS® kind DC3D8 had been used within the warmness transfer analysis.

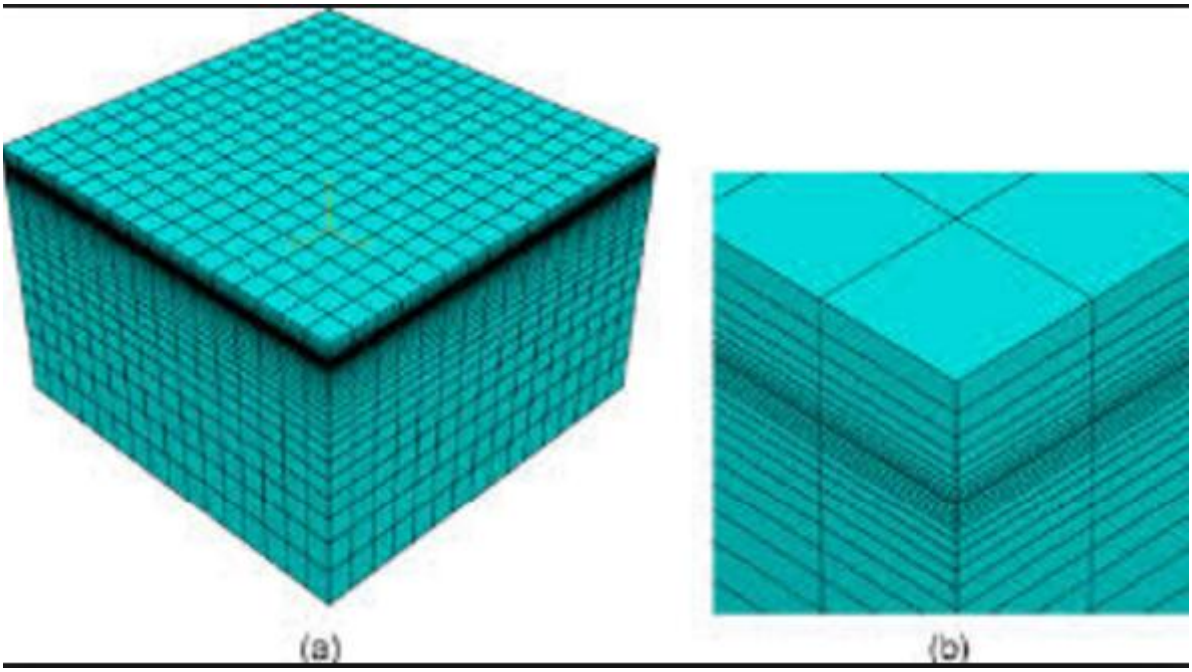


***Fig 2.*** *The 3D finite element mesh (a) Top view (b) side view*

The chemical composition of the bottom metals used on this have a look at is given in Table 2. furthermore, Temperature established thermo bodily properties, i.e., the thermal conductivity and specific warmness, are plotted in Fig. 3.

Table 2. Chemical composition of the base metals (in wt%)

| | Cr | Mo | Ni | C | Si | Mn | P | S | Fe |
|---|---|---|---|---|---|---|---|---|---|
| **2205** | 22.55 | 3.13 | 5.64 | 0.012 | 0.46 | 1.48 | 0.037 | 0.001 | Balance |
| **A36** | – | – | – | 0.088 | 0.236 | 0.627 | 0.005 | 0.025 | Balance |

Table 3. Material properties for 2205 DSS and A36 used in calculations

| Property | 2205 | A36 |
|---|---|---|
| | Value | |
| Latent heat of fusion (kJ/kg) | 500 | 247 |
| Liquidus Temperature (K) | 1773 | 1817 |
| Solidus temperature (K) | 1658 | 1738 |
| Density of metal (kg/m$^3$) | 7860 | 7760 |
| Surface emissivity | 0.7 | 0.5 |

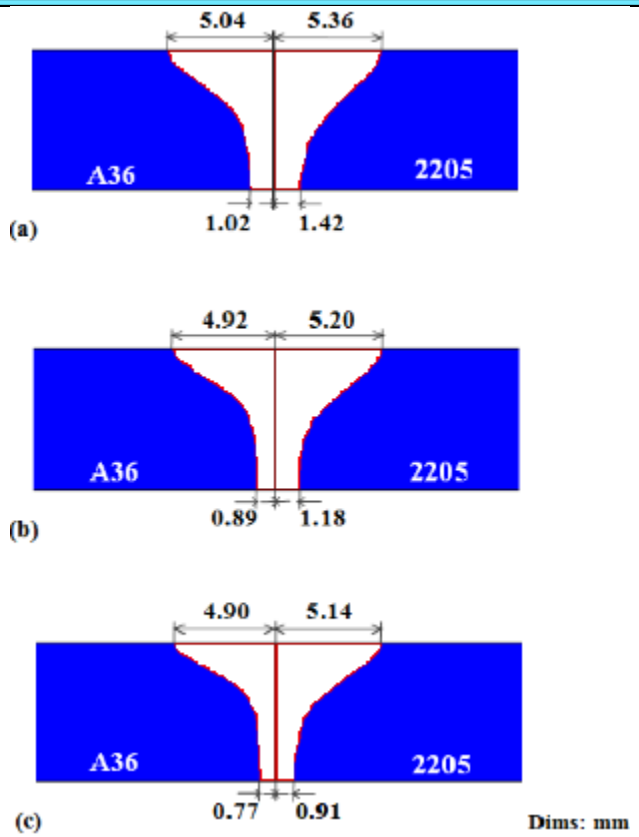


***Fig 3.*** *Numerical modeling of heat transfer and fluid flow in keyhole plasma arc welding*

**Verification of the Finite element model**

To confirm the accuracy of the thermal finite element analysis method used in the gift research, a pass keyhole PAW experiments were conducted on a 2205 DSS plate with a thickness of 6.5 mm. straight plate edges perpendicular to the plate floor had been prepared. The welding

parameters selected for the experiments have been as follows: V = 26 Volts, I = one hundred forty A, η = o.51 and a welding velocity = 0.001 mm/sec. PAW in keyhole mode was carried out without any filler metal and by means of the use of direct modern-day electrode bad (DCEN) polarity. The consequences acquired from the thermal evaluation have been in comparison with the experimental outcomes.

## Result

### Temperature Distribution

Figure 4 suggests the temperature distribut ion of the 6.8 mm thick plate when the keyhole PAW torch passes via the complete plate within the (y-course). it's far observed that every one of the material within the fusion sector rises in temperature above the melting factor, accomplishing 3623 ok for a warmness input of one.96 kJ/mm. This high temperature is the principle attribute within the formation of the keyhole, changing liquid to vapor. discern 6 indicates the evolution of the weld pool as the keyhole PAW takes area. The temperature contours imply the sample of warmth drift within the weldment. these contours are drawn for V = 28 Volts, I = a hundred and forty A, η = 0.50, and a welding speed = 0.002 mm/sec. To examine the molten-area growth, the isotherm similar to the temperature (1763 k) is plotted and tested. The absolutely developed fusion area is absolutely fashioned at (t = to + 1.15 S), has the form of a reversed bugle, the half of fusion sector width is five.20 mm at the pinnacle surface and 1.25 mm on the lowest floor for a warmth enter of one.96 kJ/mm. for this reason, the numerical consequences are in desirable settlement with the experimental measurements.

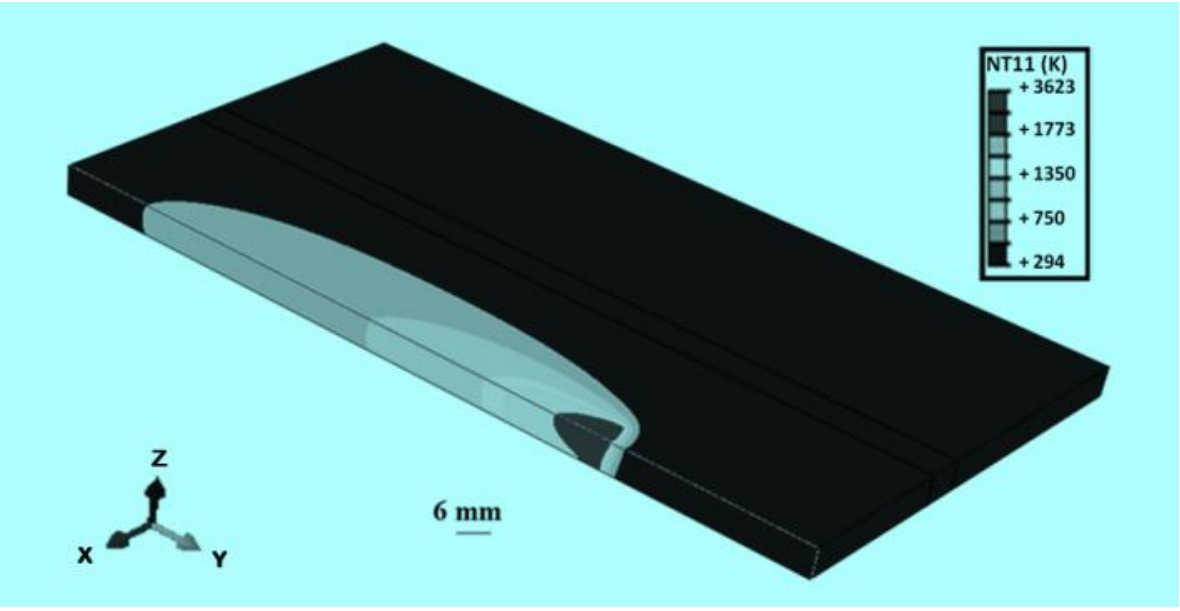


***Fig 4.*** *Three dimensional temperature distribution inside the 6.8 mm thick plate*

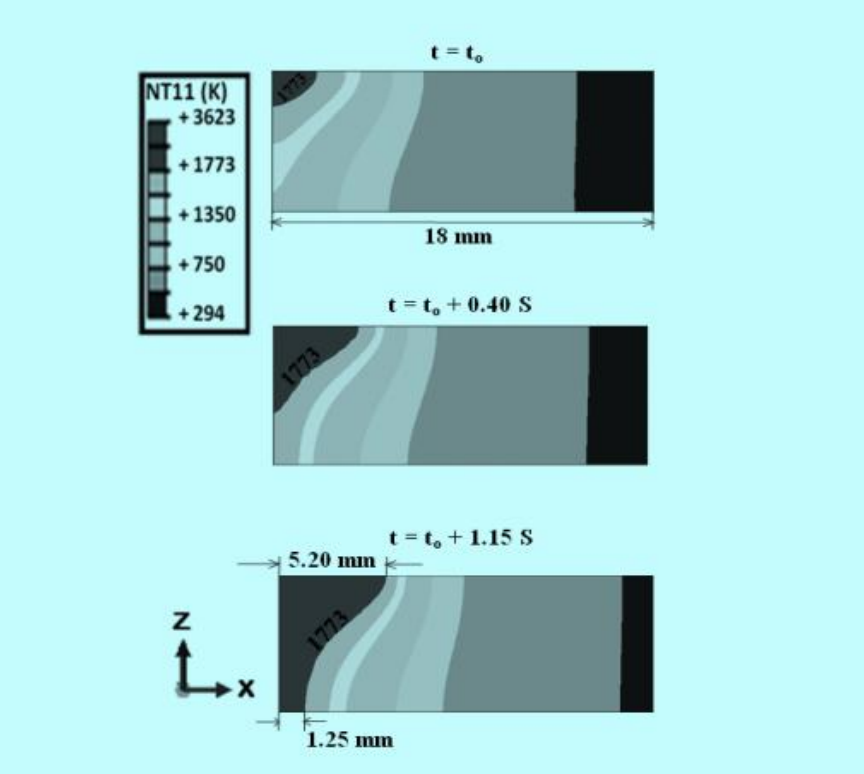


***Fig 5.*** *Isotherms in the lateral plane*

Fig. 6 displays the temperature distribution for the samples with specific welding warmth input at the center of the joint. It became located that the temperature distribution will become unsymmetrical due to the distinction of growth and shrinkage charge among duplex chrome steel (2205) and low carbon steel (A36). for the reason that low carbon metal has higher thermal expansion coefficient than duplex stainless steel. it is also located that welding heat input performs an important function in the development of weld pool form and temperature profiles. Growing the warmth enter causes an enlargement of the weld pool width. for instance, the half weld FZ width at the top surface improved via 1.15% for the duplex chrome steel facet and 0.4% for the carbon metal aspect because the welding heat input adjustments from 1.seventy five kJ/mm to 1.914 kJ/mm. even as, the 1/2 weld FZ width on the lowest floor multiplied via 22.88% for the duplex stainless-steel aspect and thirteen.48% for the carbon metallic aspect for the equal modifications within the welding warmness input. The asymmetry of the weld pool is absolutely sizeable. it is also located that flawed fusion of the substances takes vicinity during the solidification level as the method is rapid, which similar to the heat enter of 1.75 kJ/mm. consequently, using such finite detail version, it is feasible to analyze the weld fusion area size and geometry underneath any requested welding parameters.

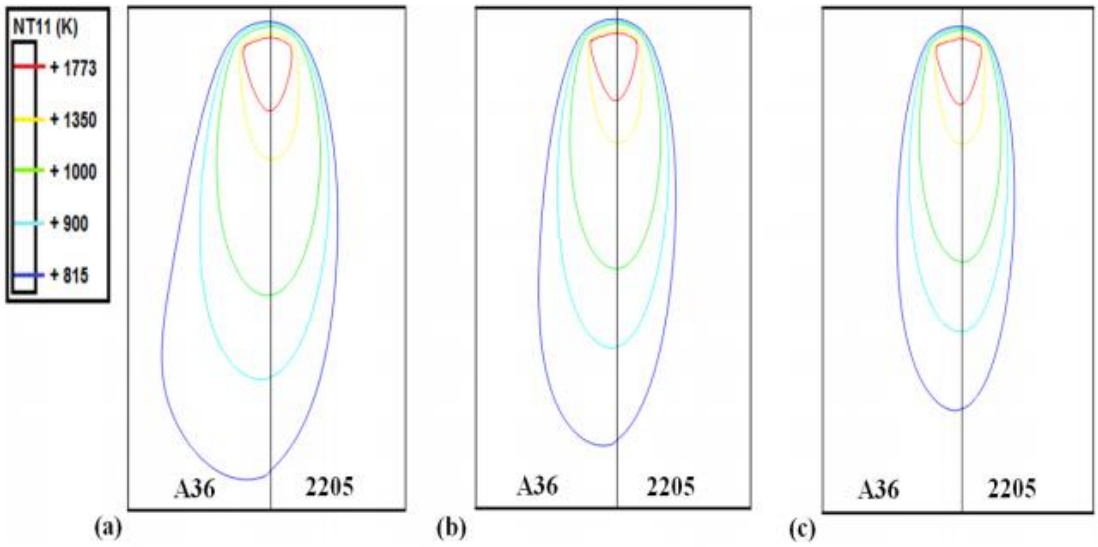


***Fig 6*** *.Isotherms on the pinnacle surface of 6.eight mm numerous 2205–A36 thick plate for a warmth input of (a) 2.25 kJ/mm, (b) 1.96 kJ/mm, and (c) 1.75 kJ/mm*

## CONCLUSIONS

The subsequent conclusions can be drawn from this evaluation:

- It's far possible to investigate the three-dimensional transient thermal analysis for the Keyhole PAW method of distinctive steels the use of the finite detail technique combined with an adaptive warmth supply version.
- A settlement has been observed among the predicted and the measured weld pool size and geometry that verify the validity of the hired version.
- The effect of fluid float and solidification of the weld pool are taken into consideration analytically; consequently, appropriate predictions of the brief isotherms and the weld pool geometry are received.
- Increasing the heat input causes an enlargement of the weld pool width. This effect is greater awesome for the duplex stainless steel aspect than the low carbon metal facet.
- If the warmth enter is decreased to1.65 kJ/mm in the keyhole PAW numerous 2205–A36 welds, there is a hazard of having wrong fusion of the materials.
- The outcomes of the constructed version may be used for the optimization of Keyhole PAW processes to acquire enough power and deep penetration.
- The results acquired can be used for future evaluation and optimization of residual stress distributions.

## REFERENCES

1. *Welding approaches manual, 1st ed., Woodhead, England, 2003, pp. 38, 39.*
2. *Urena, A., Otero, E., Utrilla, M. V., and Munez, C. J., "Weldability of a 2205 duplex stainless-steel the usage of plasma arc welding," J Mater procedure Technol, Vol. 182, No. 1-3, 2007, pp. 624–631.*
3. *Zheng, S., Dayou, P., and Ingegerd, A., "impact of twin torch method on duplex chrome steel welds," Mater Sci Eng A, Vol. 356,No. 1-2, 2003, pp. 274–282.*
4. *Taban, E., "joining of duplex chrome steel by means of plasma arc, TIG and plasma arc+TIG welding approaches," Mater Manuf system, Vol.23, No. eight, 2008, pp. 871–878.*

5. *Taban, E., "sturdiness and microstructural evaluation of high-quality duplex stainless steel joined by using plasma arc welding," J Mater Sci, Vol.43, No. 12, 2008, pp. 4309–4315.*
6. *Migiakis, okay., Daniolos, N., and Papadimitriou, G. D., "Plasma keyhole welding of americaS32760 amazing duplex stainless-steel: microstructure and mechanical residences," Mater Manuf procedure, Vol. 25, No. 7, 2010, pp. 598–605.*
7. *Barnhouse, E. J., and Lippold, J. C., "Microestructure /assets Relationships in varied Welds among Duplex Stainless Steels and Carbon Steels," Weld J, Vol. seventy seven, No. 12, 1998, pp. s477-487.*
8. *Mendoza, B. I., Maldonado, Z. C., Albiter, H. A., and Robles, P. E., "multiple Welding of Superduplex stainless-steel/HSLA steel for Offshore programs Joined through GTAW," ENG, Vol. 2, No. 7, 2010, pp. 520–528.*
9. *Keanini, R. G., and Rubinsky, B., "3-dimensional simulation of the plasma arc welding manner," Int J heat Mass switch, Vol. 36, No. 13, 1993, pp. 3283–3298.*
10. *Fan, H. G., and Kovacevic, R., "Keyhole formation and fall apart in plasma arc welding," J Phys D Appl Phys, Vol. 32, No. 22, 1999, pp. 2902–2909.*
11. *Wu, C. S., Wang, H. G., and Zhang, Y. M., "a new heat supply model for keyhole plasma arc welding in FEM evaluation of the temperature profile," Weld J, Vol eighty five, No. 12, 2006, pp. 284–291.*
12. *Wu, C. S., Hu, Q. X., and Gao, J. Q., "An adaptive heat supply model for finite-detail analysis of keyhole plasma arc welding," Comput Mater Sci, Vol. forty six, No. 1, 2009, pp. 167–172.*
13. *Wang, H. X., Wei, Y. H., and Yang, C. L., "Numerical simulation of variable polarity vertical-up plasma arc welding process," Comput Mater Sci, Vol. 38, No. four, 2007, pp. 571–587.*
14. *ABAQUS person's guide, model 6.10, Karlsson & Sorensen, Inc., Hibbitt, 2010.*
15. *Labudovic, M., Hu, D., and Kovacevic, R., "3-dimensional finite detail modelling of laser floor change," I Mech E, Vol. 214, No. eight, 2000, pp. 683–692.*
16. *Punitharani, okay., Murugan, N., and Sivagamai, S. M., "Finite detail analysis of residual stresses and distortion in difficult confronted gate valve," J Sci Ind Res, Vol. sixty nine, No. 2, 2010, pp. 129–134.*
17. *Jiang, W., Yahiaoui, okay., hall, F. R., and Laoui, T., "Finite element simulation of multipass welding: full three-dimensional as opposed to generalized plane pressure or axisymmetric models," J pressure analysis, Vol. 40, No. 6, 2005, pp. 587–597.*
18. *Deng, D., and Murakawa, H., "Numerical simulation of temperature area and residual strain in multi-bypass welds in stainless-steel pipe and evaluation with experimental measurements," Comput Mater Sci, Vol. 37, 2006, pp. 269–277.*
19. *Deng, D., and Murakawa, H., "Finite element analysis of temperature area, microstructure and residual pressure in multi-pass buttwelded 2.25Cr–1Mo metal pipes," Comput Mater Sci, Vol. 43, 2008, pp. 681–695.*
20. *Abid, M., and Qarni, M. J., "3D thermal finite detail evaluation of single bypass girth welded low carbon metal pipe-flange joints," Turkish J Eng Env Sci, Vol. 33, 2009, pp. 1–13.*
21. *Bonifaz, E. A., and Richards, N. L., "Modeling forged IN-738 superalloy*

*gas tungsten arc welds," Acta Materialia, Vol. fifty seven, 2009, pp. 1785–1794.*

22. *Deng, D., "FEM prediction of welding residual strain and distortion in carbon steel considering section transformation effects," Mater and Des, Vol. 30, 2009, pp. 359–366.*